THE RESPONSE OF A SINGLE WALL SPACE STRUCTURE TO IMPACT BY COMETARY METEOROIDS OF VARIOUS SHAPES

By

Robert J. Hayduk

Thesis submitted to the Graduate Faculty of the

Virginia Polytechnic Institute

in candidacy for the degree of

MASTER OF SCIENCE

in

Engineering Mechanics

May 1968

THE RESPONSE OF A SINGLE WALL SPACE STRUCTURE TO IMPACT BY COMETARY METEOROIDS OF VARIOUS SHAPES

By

Robert J. Hayduk

Thesis submitted to the Graduate Faculty of the

Virginia Polytechnic Institute

in partial fulfillment for the degree of

MASTER OF SCIENCE

in

Engineering Mechanics

APPROVED:

Chairman, G. W. Swift

D. Frederick

D. H. Pletta, Head
Engineering Mechanics
Department

C. W. Smith

May 1968

Blacksburg, Virginia

II. TABLE OF CONTENTS

III. ACKNOWLEDGMENTS

The author is grateful to the National Aeronautics and Space Administration for permitting him to write this thesis at the Langley Research Center; to Engineering Mechanics Department, Virginia Polytechnic Institute, for his comments and guidance; and to Mathematician, Langley Research Center, for performing the computational programing.

IV. LIST OF FIGURES

V. INTRODUCTION

The literature indicates general concern over the hazard of travel in the meteoroid environment of space. Catastrophic failures of manned and unmanned space vehicles can result from meteoroid penetration of an underdesigned spacecraft hull. The National Aeronautics and Space Administration is investigating the reactions of space structures subjected to impact by hypervelocity projectiles. These investigations along with added knowledge of the meteoroid environment are continually upgrading the spacecraft design equations.

Present laboratory simulation capabilities are barely reaching the lower limit of the meteoroid velocity range with moderately large projectiles. Since space structures cannot be subjected to an extensive simulation of the environment, any design equation can only receive limited verification before being extended to the environment. Any analytical model, then, should be as realistic as possible in the approximation of the hypervelocity phenomenon of meteoroid impact.

This thesis presents an analytical model of the hypervelocity impact between an axisymmetric cometary meteoroid and a single wall space structure. Linear, small-deflection plate theory is used to study the stress at the contact axis and the deflection of the single wall.

Classical plate theory has been used by many investigators to study the response of plates to projectile impact. Reference 1 contains solutions to impulsively loaded infinite plate problems frequently referenced in the literature. Particular problems are an impulsive point force at the origin, an impulsive force uniformly distributed over a circle, and

an impulsive Gaussian distribution of pressure. In reference 2, the deflections away from the impact point of a large plate centrally impacted by a bullet agreed after a short time with those obtained by mathematically simulating the impact by an impulsive point force of finite duration on an infinite plate. Also presented in reference 2 are solutions to the impulsive point force problem for various time functions: finite duration, step function, and unit impulse function.

The hypervelocity impact between a right circular cylinder and a thin elastic plate was analyzed in reference 3. It was assumed that the projectile gave the contact portion of the plate a uniform initial velocity determined from conservation of momentum. The stress at the axis of symmetry was used as an indicator of the failure threshold to obtain a simple ballistic limit thickness expression. The analysis presented here was performed using an approach similar to that used in reference 3, but generalizes the problem to any axisymmetric projectile. The displacement of the single wall and the time variation of the stress at the origin are investigated. Solutions for three particular projectiles - cylinder, cone, and sphere - are presented for comparison.

VI. SYMBOLS

a	radius of contact between projectile and plate
$B(x,y)$	beta function
c	speed of sound in plate material, $\sqrt{E/\rho_t}$
D	flexural rigidity of the plate, $Eh^3/12(1 - \nu^2)$
E	elastic modulus of plate material in tension and compression
e	strain
F	hypergeometric function
g	projectile functional
h	target thickness
J	Bessel function
$K = \frac{2a^2}{ch}\sqrt{3(1 - \nu^2)}$	
M	bending moment resultant
ℓ	projectile length
p	Hankel transform parameter
$Q = K\frac{\rho_p}{\rho_t}\frac{V_p}{h}$	
r	radial coordinate
t	time
V	velocity
$w(\eta,t)$	transverse displacement of the plate's midplane
$\eta = \frac{r}{a}$	
ν	Poisson's ratio
ρ	density

σ stress

$\tau = \frac{t}{K}$

Subscripts

t target

p projectile

co cone

cyl cylinder

r radial

sph sphere

θ tangential

μ indicates order of Bessel function

ν indicates order of Bessel function

Superscripts

$\cdot$ derivative with respect to time

$\sim$ nondimensional

$-$ transform

$=$ nondimensional equi-mass and -diameter

μ indicates order of Bessel function

ν indicates order of Bessel function

VII. MATHEMATICAL DEVELOPMENT OF THE PROBLEM

Transformed Governing Equation and General Solution

The governing equation for the bending of a thin plate from linear, elastic, small-deflection theory is

$$\nabla^4 w = -K^2 \frac{\partial^2 w}{\partial t^2} \tag{1a}$$

where

$$K = \frac{2a^2}{ch} \sqrt{3(1 - \nu^2)} \tag{1b}$$

and the operator in polar coordinates is

$$\nabla^4 = \left[\frac{1}{\eta} \frac{\partial}{\partial \eta}\left(\eta \frac{\partial}{\partial \eta}\right)\right]\left[\frac{1}{\eta} \frac{\partial}{\partial \eta}\left(\eta \frac{\partial}{\partial \eta}\right)\right] \tag{1c}$$

$w(\eta,t)$ is the transverse displacement of the midplane of the plate, a is the impacting projectile radius, c is the speed of sound in the plate material, h is the plate thickness, ν is Poisson's ratio, and η is the radial coordinate r divided by the projectile radius.

Having conveniently selected the plate as infinite in extent makes the problem amenable to a zeroth order Hankel transform in the nondimensional radial coordinate η. The forward and inverse transforms are, respectively,

$$\bar{f}(p) = \int_0^\infty \eta f(\eta) J_0(p\eta) d\eta \tag{2a}$$

$$f(\eta) = \int_0^\infty p\bar{f}(p)J_o(p\eta)dp \tag{2b}$$

Multiplying the governing equation (1a) by $\eta J_o(p\eta)$ and integrating with respect to η by parts several times yields the following result:

$$\left\{\eta J_o(p\eta)\,\frac{\partial}{\partial\eta}\left[\frac{1}{\eta}\,\frac{\partial}{\partial\eta}\left(\eta\,\frac{\partial w}{\partial\eta}\right)\right] + p\,\frac{\partial}{\partial\eta}\left(\eta\,\frac{\partial w}{\partial\eta}\right)J_1(p\eta) - p^2\eta\,\frac{\partial w}{\partial\eta}\,J_o(p\eta) - p^3 w\eta J_1(p\eta)\right\}_{\eta=0}^{\infty} + K^2\,\frac{d^2\bar{w}}{dt^2} + p^4\bar{w} = 0 \tag{3}$$

If the boundary conditions of zero deflection, slope, and shear per unit length at infinity and zero slope and finite shear at the origin are assumed and coupled with the kernel of the transformation, the term in brackets vanishes. If the time is nondimensionalized to $\tau = \frac{t}{K}$, the transformed differential equation becomes

$$\frac{d^2\bar{w}}{d\tau^2} + p^4\bar{w} = 0 \tag{4}$$

with general solution

$$\bar{w}(p,\tau) = A(p)\sin(p^2\tau) + B(p)\cos(p^2\tau) \tag{5}$$

Applying the zero deflection initial condition ($\bar{w}(p,0) = 0$) indicates that $B(p)$ must be zero. The coefficient $A(p)$ is determinable from the transform of the initial target velocity, that is,

$$\dot{\bar{w}}(p,t) = \frac{1}{K}\frac{\partial \bar{w}(p,\tau)}{\partial \tau}$$

$$= \frac{1}{K} p^2 A(p)\cos(p^2\tau)$$

Therefore,

$$A(p) = Kp^{-2}\dot{\bar{w}}(p,0) \qquad (6)$$

Determination of Initial Plate Velocity

(Cometary Meteoroid Impact Model)

Reference 4 summarizes the interplanetary meteoroid environment as consisting of debris in two distinct forms: hard, dense asteroidal particles in relatively sparse quantities and porous, fragile cometary particles constituting almost 100 percent of the total. These cometary meteoroids, as described in reference 5, are thought to have a density on the order of 0.5 gm/cm^3 and extremely low crushing strength such as cigar ash.

Upon impact with a structure at a velocity between 11 and 72 km/sec, a cometary meteoroid is assumed to act as a projectile consisting of discrete small particles which interact negligibly since the crushing strength is so low. This leads to a model of continuous momentum exchange during impact if the further assumption is made that a momentum balance is of primary importance. This time variation of the loading, so to speak, is extremely difficult to include in an analysis. Therefore, this model will assume the worst case - all the momentum of the cometary meteoroid impacts instantaneously.

Any axisymmetric projectile will be represented in the analysis by the function representing its total momentum projected onto the plate rather than the analytic expression for its shape. Figure 1 illustrates this point for a sphere. The upper diagram shows a sphere and its analytic expression

$$z = a\left(1 \pm \sqrt{1 - \eta^2}\right) \tag{7}$$

The lower diagram shows the functional representing the total projected momentum per unit area of the sphere, that is,

$$f_{sph}(\eta) = 2a\sqrt{1 - \eta^2} \tag{8}$$

Hence, the momentum impacting an annular ring of radius η and width $d\eta$ is

$$2\pi a^2 \eta\, d\eta\, f_p(\eta) V_p \rho_p \tag{9}$$

Balancing momentum between the projectile and target yields the initial velocity of the target as

$$\dot{w}(\eta,0) = \begin{cases} \left(\dfrac{\rho_p}{\rho_t}\right)\left(\dfrac{V_p}{h}\right) f_p(\eta); & 0 < \eta < 1 \\ 0 \qquad\qquad\qquad\quad ; & 1 < \eta < \infty \end{cases} \tag{10}$$

where the momentum of the projectile has been neglected after impact.

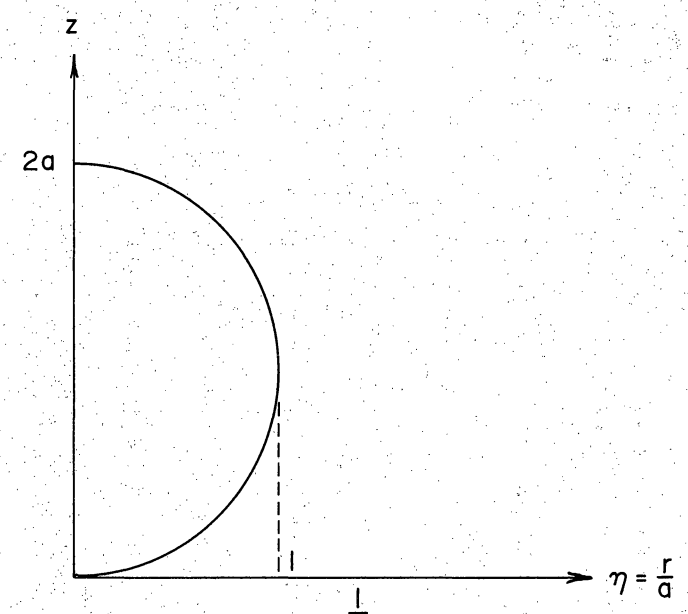

Geometric Equation: $z = a\left[1 \pm (1-\eta^2)^{\frac{1}{2}}\right]$

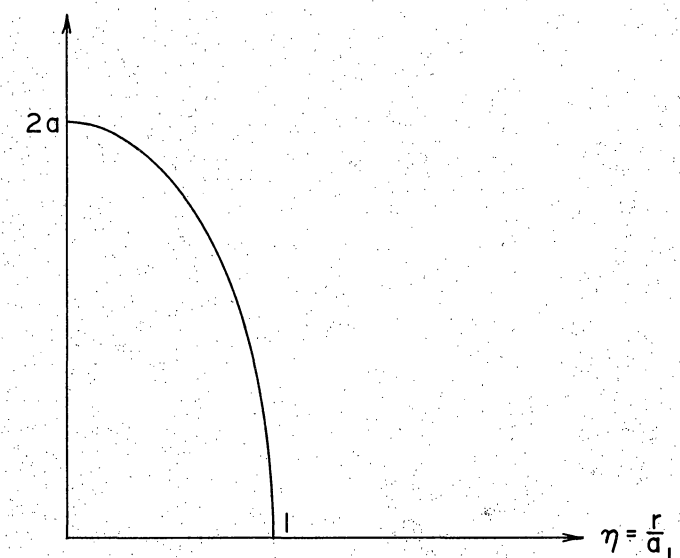

Momentum Per Unit Area Functional: $f_{sph}(\eta) = 2a(1-\eta^2)^{\frac{1}{2}}$

Figure 1.- Comparison of the sphere's geometric equation and functional form of the projected momentum per unit area.

Transforming this initial velocity evaluates the coefficient $A(p)$ (eq. (6)) as

$$A(p) = Q l_p p^{-2} \int_0^1 \eta g_p(\eta) J_o(p\eta) d\eta$$

$$= Q l_p p^{-2} \bar{g}_p(p) \qquad (11)$$

where the nondimensional quantity $K \frac{\rho_p}{\rho_t} \frac{V_p}{h}$ has been represented by Q, and the functional $f_p(\eta)$ has been represented by a characteristic length, l_p, times another functional $g_p(\eta)$.

VIII. MATHEMATICAL SOLUTION OF THE PROBLEM

Displacement of the Plate

Substituting equation (11) and $B(p) = 0$ into equation (5) and inverting according to equation (2b) yields the displacement of the plate in integral form as

$$w_p(\eta,\tau) = Q\ell_p \int_o^\infty p^{-1}\bar{g}_p(p)J_o(p\eta)\sin(p^2\tau)dp \tag{12a}$$

or dividing by $Q\ell_p$ to nondimensionalize yields

$$\tilde{w}_p(\eta,\tau) = \int_o^\infty p^{-1}\bar{g}_p(p)J_o(p\eta)\sin(p^2\tau)dp \tag{12b}$$

Stresses, Strains, and Bending Moment Resultants at the Origin

From linear, elastic plate theory, the appropriate equations for stress, strain, bending moment resultants, and shear stress resultant are, respectively,

$$\sigma_{rr} = -\frac{zE}{a^2(1-\nu^2)}\left\{\frac{\partial^2 w}{\partial\eta^2} + \frac{\nu}{\eta}\frac{\partial w}{\partial\eta}\right\} \tag{13a}$$

$$\sigma_{\theta\theta} = -\frac{zE}{a^2(1-\nu^2)}\left\{\frac{1}{\eta}\frac{\partial w}{\partial\eta} + \nu\frac{\partial^2 w}{\partial\eta^2}\right\} \tag{13b}$$

$$e_{rr} = -\frac{z}{a^2}\frac{\partial^2 w}{\partial\eta^2} \tag{14a}$$

$$e_{\theta\theta} = -\frac{z}{a^2}\frac{1}{\eta}\frac{\partial w}{\partial\eta} \tag{14b}$$

$$M_r = - \frac{D}{a^2} \left\{ \frac{\partial^2 w}{\partial \eta^2} + \frac{\nu}{\eta} \frac{\partial w}{\partial \eta} \right\} \tag{15a}$$

$$M_\theta = - \frac{D}{a^2} \left\{ \frac{1}{\eta} \frac{\partial w}{\partial \eta} + \nu \frac{\partial^2 w}{\partial \eta^2} \right\} \tag{15b}$$

$$Q_r = - \frac{D}{a^3} \frac{\partial}{\partial \eta} (\nabla^2 w) \tag{16}$$

where the remaining quantities are zero because of thin plate assumptions and the axisymmetry of the problem.

Due to symmetry and the monotonically decreasing projectile shape the maximum stress, strain, and bending moment resultants occur at the axis of symmetry. Knowledge of these maximum plate responses is essential for hypervelocity impact studies of spacecraft with protection of the occupants (both equipment and people) in mind.

At the axis of symmetry (origin of coordinate system), both the radial and circumferential stresses, strains, and bending moment resultants are identical because

$$\lim_{\eta \to 0} \frac{1}{\eta} \frac{\partial w}{\partial \eta} = \left. \frac{\partial^2 w}{\partial \eta^2} \right|_{\eta=0} \tag{17}$$

by l'Hospital's rule. Thus, the nondimensional stress, strain, and bending moment resultants are identical at the origin, that is,

$$\tilde{\sigma} = \tilde{e} = \tilde{M} = - \left. \frac{\partial^2 \tilde{w}}{\partial \eta^2} \right|_{\eta=0} \tag{18}$$

where

$$\tilde{\sigma} = \frac{a^2(1-\nu)}{zEQl_p}\left[\sigma_{rr} \text{ or } \sigma_{\theta\theta}\right]_{\eta=0} \tag{19}$$

$$\tilde{e} = \frac{a^2}{zQl_p}\left[e_{rr} \text{ or } e_{\theta\theta}\right]_{\eta=0} \tag{20}$$

$$\tilde{M} = \frac{a^2}{D(1+\nu)Ql_p}\left[M_r \text{ or } M_\theta\right]_{\eta=0} \tag{21}$$

Before differentiating the displacement (eq. (12b)) to evaluate the stress at the origin, substitute the integral expression (eq. (11)) for $\bar{g}_p(p)$ and switch the order of integration to get

$$\tilde{w}_p(\eta,\tau) = \int_0^1 ug_p(u)du \int_0^\infty p^{-1}J_0(pu)J_0(p\eta)\sin(p^2\tau)dp \tag{22}$$

Differentiating twice with respect to η and letting η go to zero gives

$$\left.\frac{\partial^2\tilde{w}_p}{\partial\eta^2}\right|_{\eta=0} = -\frac{1}{2}\int_0^1 ug_p(u)du \int_0^\infty pJ_0(pu)\sin(p^2\tau)dp \tag{23}$$

and the stress at the origin (eq. (18)) can be written as

$$\tilde{\sigma}_p = \frac{1}{2}\int_0^1 ug_p(u)du \int_0^\infty pJ_0(pu)\sin(p^2\tau)dp \tag{24}$$

After evaluation of the infinite integral (see appendix), the stress at the origin reduces to a single definite integral, that is,

$$\tilde{\sigma}_p = \frac{1}{4\tau} \int_0^1 u g_p(u) \cos\left(\frac{u^2}{4\tau}\right) du; \quad \tau \neq 0 \tag{25}$$

which can be integrated once $g_p(u)$ is known for the particular axisymmetric projectile.

IX. PARTICULAR SOLUTIONS FOR CYLINDRICAL, CONICAL, AND SPHERICAL PROJECTILES

The three particular axisymmetric projectiles to be studied are the usual ones used in hypervelocity laboratories - cylinder, cone, and sphere - even though the analysis is not intended for the high-strength, high-density laboratory projectiles. Since it is assumed that the total momentum of the projectile is imparted to the plate instantaneously, this analysis does not distinguish between the conical projectile (or any other projectile for that matter) impacting base down from the same projectile impacting apex down.

Figure 2 presents the three particular axisymmetric projectiles and their functional representation in the analysis.

Displacement of the Plate

Cylinder.- $g_{cyl}(\eta) = 1$

Substituting $g_{cyl}(\eta) = 1$ into equation (11) yields

$$\bar{g}_{cyl}(p) = \int_0^1 uJ_0(pu)du$$

$$= p^{-1}J_1(p) \qquad (26)$$

The nondimensional displacement (eq. (12)) for the cylindrical projectile thus becomes

$$\tilde{w}_{cyl}(\eta,\tau) = \int_0^\infty p^{-2}\, J_1(p)J_0(p\eta)\sin(p^2\tau)dp \qquad (27)$$

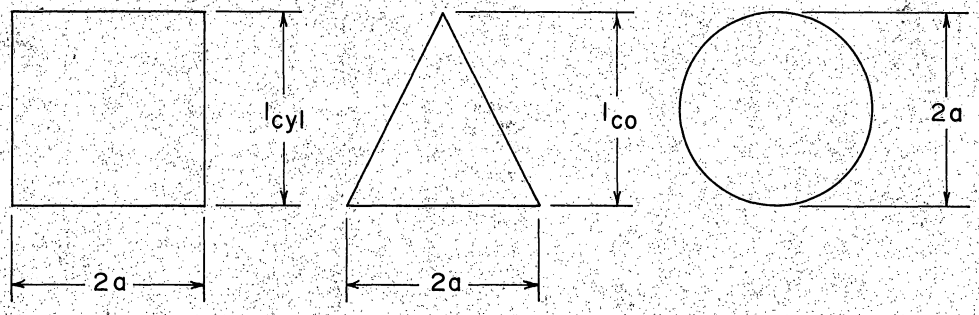

Projectile :	Cylinder	Cone	Sphere
$f_p(\eta)=l_p\, g_p(\eta)$:	$l_{cyl}(1)$	$l_{co}(1-\eta)$	$2a(1-\eta^2)^{\frac{1}{2}}$

Figure 2.- Specific projectile shapes studied and their mathematical representation in the analysis.

Cone.- $g_{co}(\eta) = 1 - \eta$

Substituting $g_{co}(\eta) = 1 - \eta$ into equation (11) yields

$$\bar{g}_{co}(p) = \int_o^1 uJ_o(pu)du - \int_o^1 u^2 J_o(pu)du$$

$$= p^{-1} J_1(p) - \frac{1}{3} {}_1F_2\left(\frac{3}{2};1,\frac{5}{2};-\frac{1}{4}p^2\right) \tag{28}$$

(see appendix for evaluation of second integral) which when substituted into equation (12) gives the nondimensional displacement of the plate for the conical projectile as

$$\tilde{w}_{co}(\eta,\tau) = \int_o^\infty p^{-2} J_1(p)J_o(p\eta)\sin(p^2\tau)dp$$

$$- \frac{1}{3} \int_o^\infty p^{-1} {}_1F_2\left(\frac{3}{2};1,\frac{5}{2};-\frac{1}{4}p^2\right)J_o(p\eta)\sin(p^2\tau)dp \tag{29}$$

The first integral represents the deflection of the plate due to a cylindrical projectile of the same length as the cone, and the second integral represents the correction necessary to account for the cone's taper.

Sphere.- $g_{sph}(\eta) = (1 - \eta^2)^{1/2}$

Substituting $g_{sph}(\eta) = (1 - \eta^2)^{1/2}$ into equation (11) yields

$$\bar{g}_{sph}(p) = \int_o^1 u(1 - u^2)^{1/2} J_o(pu)du$$

$$= \left(\frac{\pi}{2}\right)^{1/2} p^{-3/2} J_{3/2}(p) \tag{30}$$

(see appendix for evaluation of this integral) which when substituted into equation (12) gives the nondimensional displacement of the plate for the spherical projectile as

$$\tilde{w}_{sph}(\eta,\tau) = \left(\frac{\pi}{2}\right)^{1/2} \int_0^\infty p^{-5/2} J_{3/2}(p) J_o(p\eta) \sin(p^2\tau) dp \qquad (31)$$

The sine function in the integrands of equations (27), (29), and (31) can be approximated for $\tau \ll 1$ by the first term of the sine series, that is,

$$\sin p^2\tau \approx p^2\tau$$

This substitution renders the short time displacements for the three cases integrable (see appendix) yielding for the cylinder

$$\tilde{w}_{cyl}(\eta,\tau \ll 1) = \begin{cases} \tau; & 0 < \eta < 1 \\ 0; & 1 < \eta < \infty \end{cases} \qquad (32)$$

for the cone

$$\tilde{w}_{co}(\eta,\tau \ll 1) = \begin{cases} \tau(1 - \eta); & 0 < \eta < 1 \\ 0 \quad\quad ; & 1 < \eta < \infty \end{cases} \qquad (33)$$

and for the sphere

$$\tilde{w}_{sph}(\eta,\tau \ll 1) = \begin{cases} \tau(1 - \eta^2)^{1/2}; & 0 < \eta < 1 \\ 0 \quad\quad\quad ; & 1 < \eta < \infty \end{cases} \qquad (34)$$

For very short time, then, the deflection of the plate is linear in time, is confined to that portion of the plate impacted, and has the shape of the projected momentum per unit area of the projectile.

Thus far, in the three examples, only projectile shape has been specified. To make realistic comparisons of the plate's deflection at various times, select projectiles of equal mass and diameter. The characteristic lengths then will be $l_{cyl} = \frac{4}{3}a$, $l_{co} = 4a$, and $l_{sph} = 2a$. The comparable nondimensional deflections can be written as

$$\bar{\bar{w}}_{cyl} = \frac{w_{cyl}}{2aQ} = \frac{2}{3}\tilde{\tilde{w}}_{cyl} \tag{35a}$$

$$\bar{\bar{w}}_{co} = \frac{w_{co}}{2aQ} = 2\tilde{\tilde{w}}_{co} \tag{35b}$$

$$\bar{\bar{w}}_{sph} = \frac{w_{sph}}{2aQ} = \tilde{\tilde{w}}_{sph} \tag{35c}$$

The short time displacements of the plate for comparable projectiles are plotted in figure 3. Figures 4 through 7 present plate deflections at $\tau = 0.15$, 0.4, 0.6, and 1.0, respectively. As early as $\tau = 0.15$ the shape of the projected momentum per unit area of the projectile is no longer evident in the plate's deflection. As time increases, the velocity of the plate origin decreases faster than at positions away from the origin and a flexural wave moves radially outward.

The maximum deflection ($\eta = 0$ in eqs. (32), (33), and (34) combined with eqs. (35a), (35b), and (35c)) at a particular time ($\tau \ll 1$) due to the cone impact is three times and due to the sphere is one and one-half times that for the cylinder. As early as $\tau = 0.15$ these large

a. Cylinder projectile

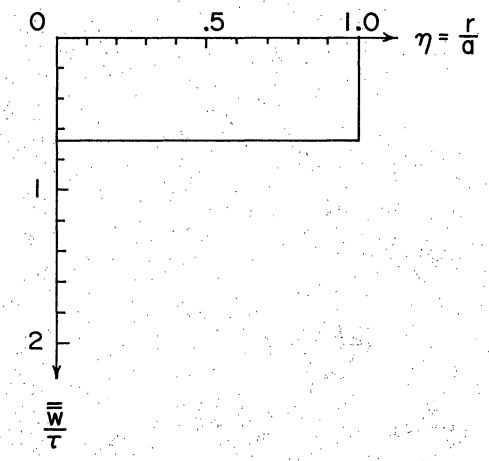

b. Cone projectile

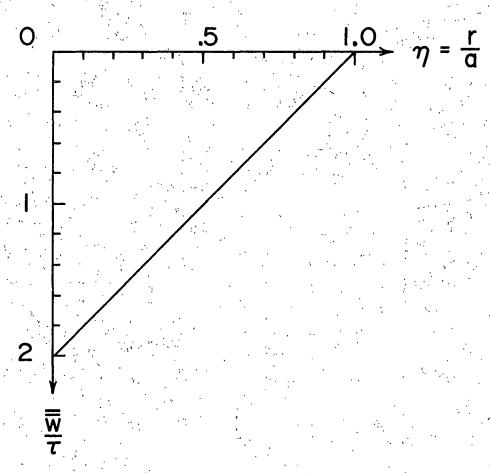

c. Sphere projectile

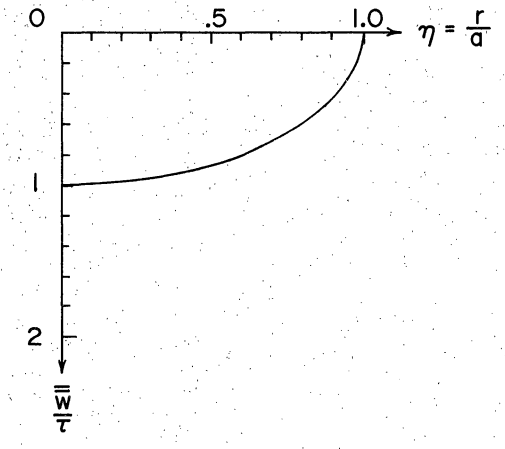

Figure 3.- Short time deflection of the plate ($\tau \ll 1$).

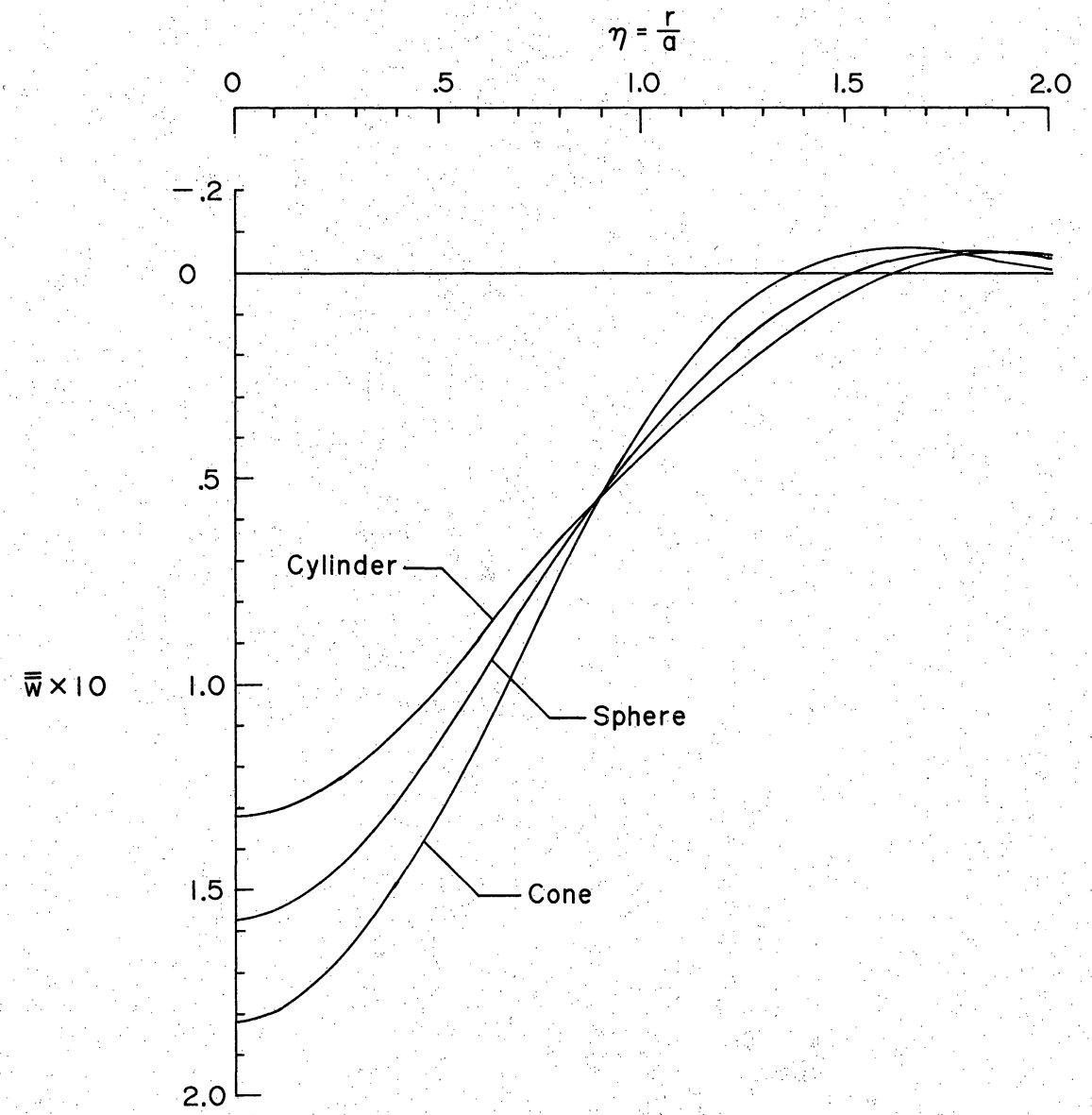

Figure 4.- Comparison of the plate's deflection at $\tau = 0.15$ for impacting equi-mass and -diameter projectiles.

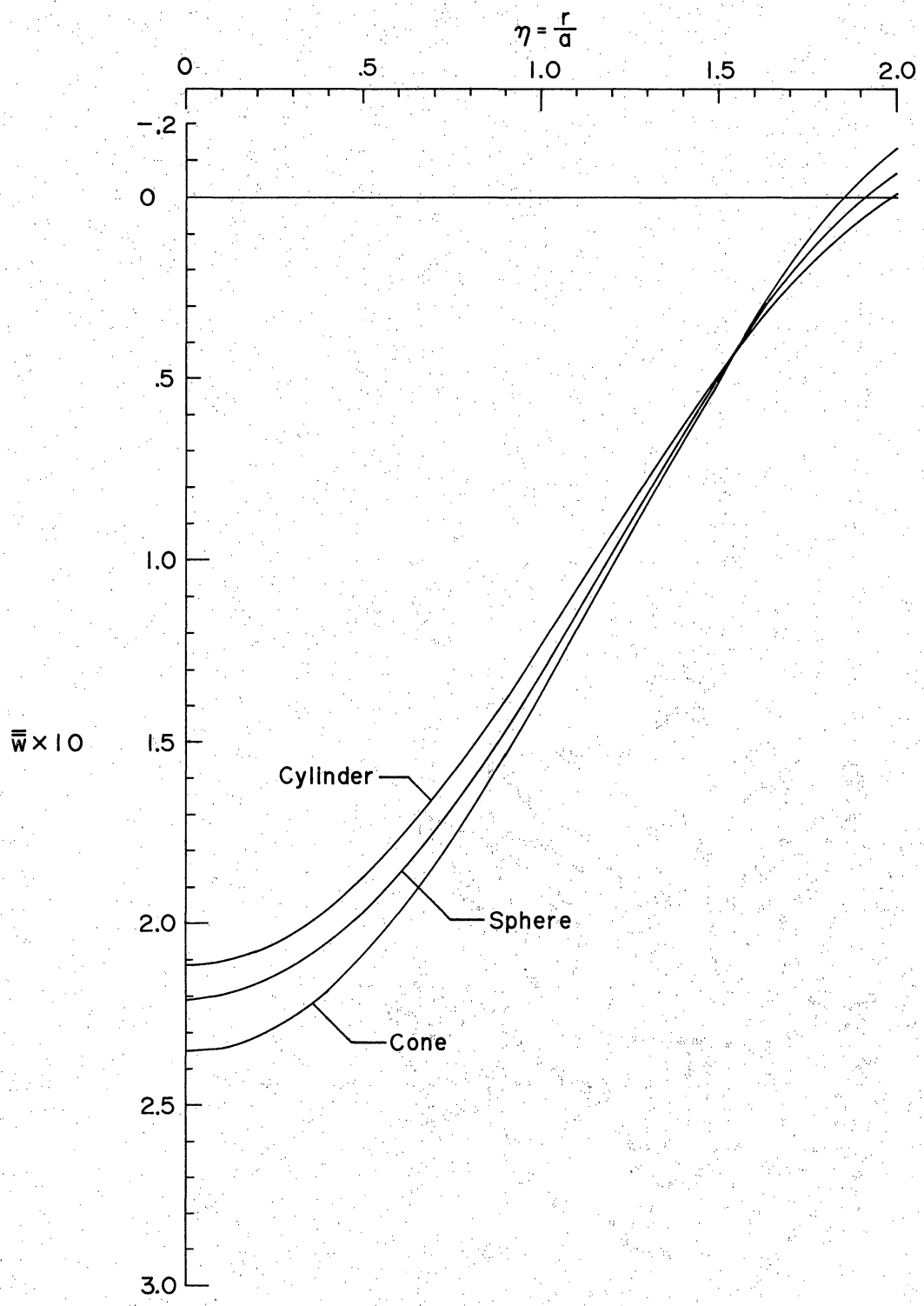

Figure 5.- Comparison of the plate's deflection at $\tau = 0.4$ for impacting equi-mass and -diameter projectiles.

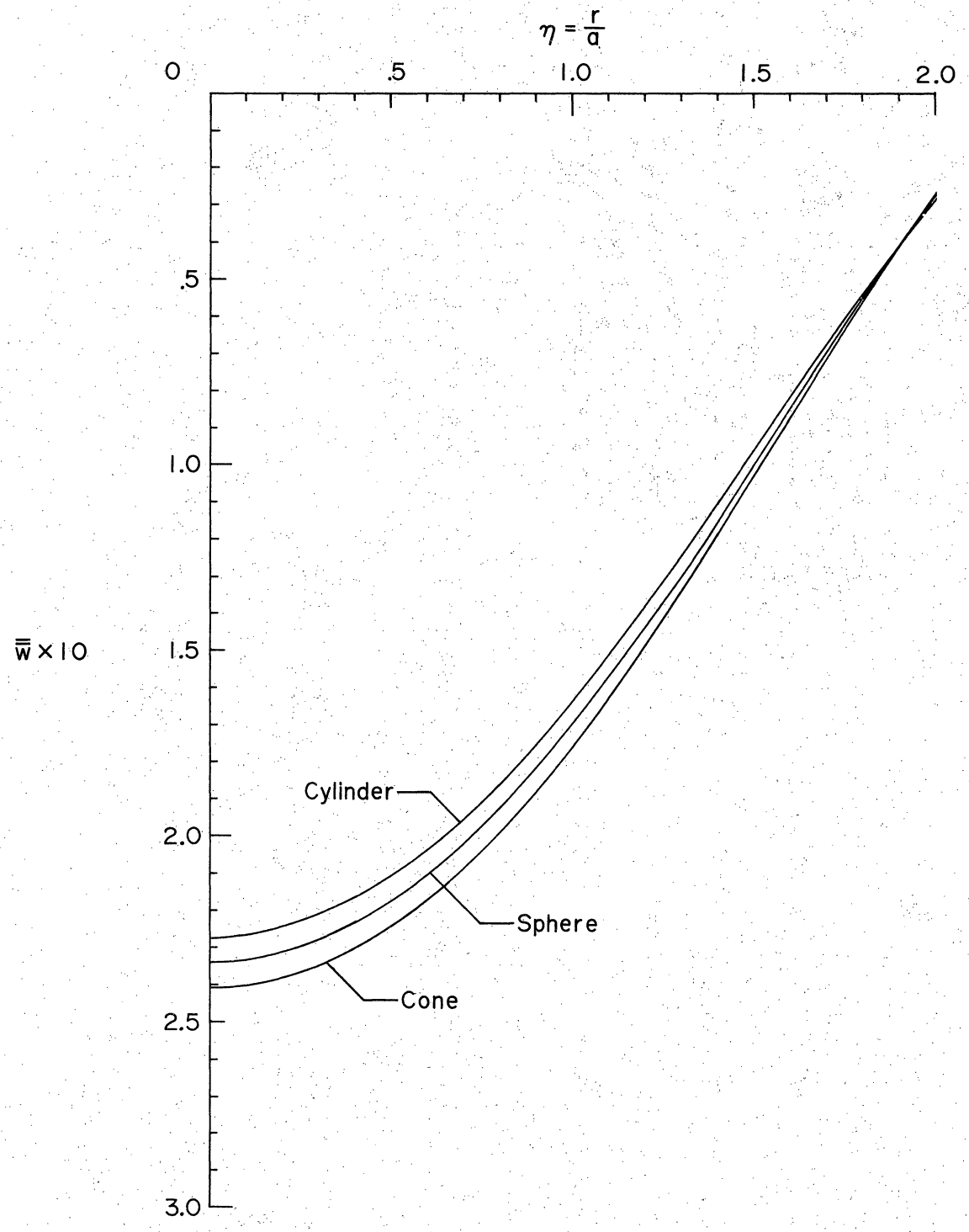

Figure 6.- Comparison of the plate's deflection at $\tau = 0.6$ for impacting equi-mass and -diameter projectiles.

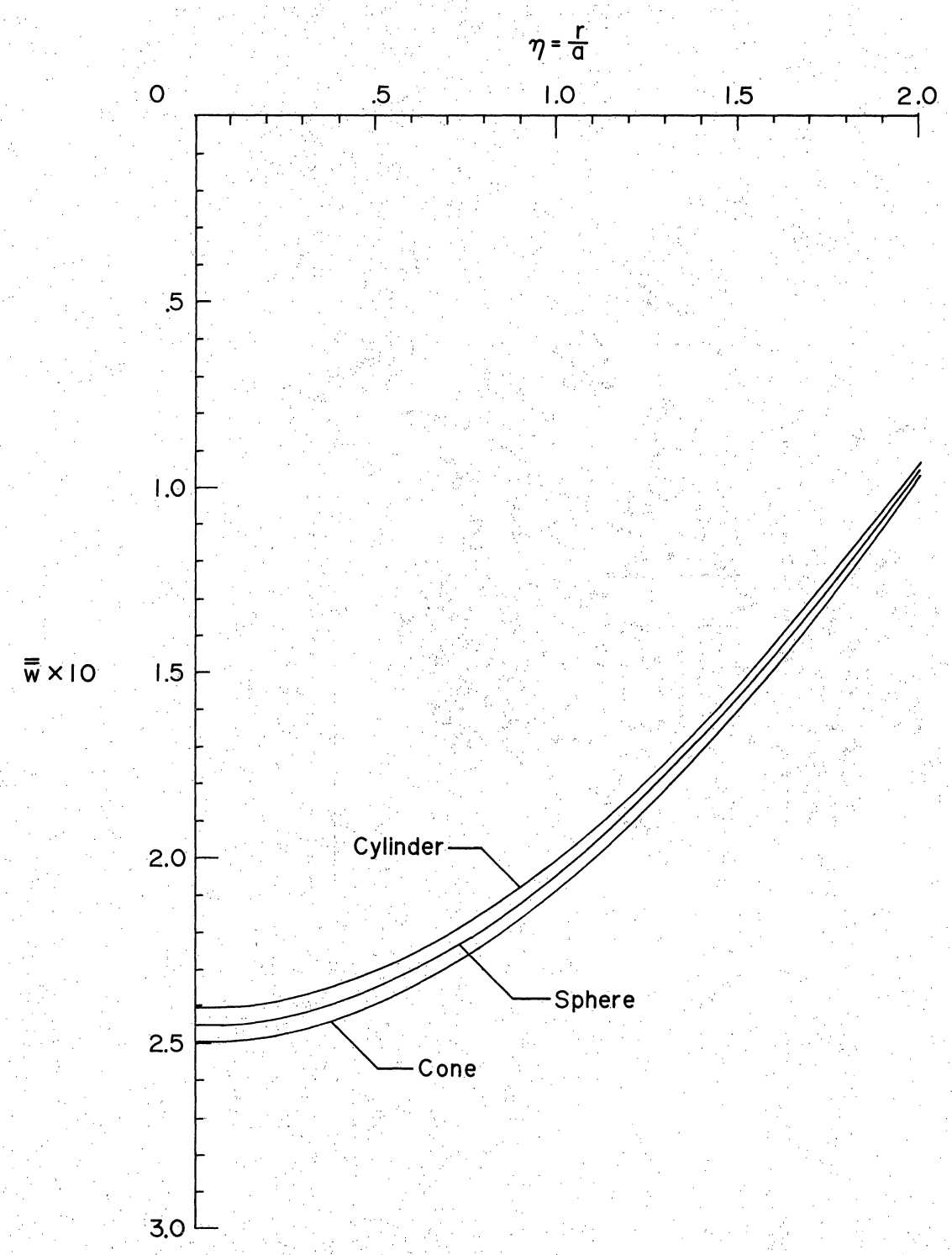

Figure 7.- Comparison of the plate's deflection at $\tau = 1.0$ for impacting equi-mass and -diameter projectiles.

differences in deflection have drastically diminished $\left(\frac{\bar{\bar{w}}_{co}}{\bar{\bar{w}}_{cyl}} = 1.37 \text{ and } \frac{\bar{\bar{w}}_{sph}}{\bar{\bar{w}}_{cyl}} = 1.18\right)$ as shown in figure 4. By $\tau = 1.0$ the deflection of the plate is nearly the same for all three projectile impacts.

The short time and $\tau = 0.15$ plate deflection curves indicate that the cone projectile causes the largest deflection at early times after impact. The sphere causes correspondingly less deflection of the plate than the cone, but more than the cylinder.

Maximum Stress for Specific Cases

Since the maximum stress, strain, and bending moment resultants have been shown to be of the same functional form, the discussion will be restricted to maximum stress with the understanding that the comments are applicable also to the maximum strain and maximum bending moment resultant.

Cylinder.- $g_{cyl}(\eta) = 1$

Recalling equation (25) and $g_{cyl}(\eta) = 1$, the nondimensional stress at the origin for the cylindrical projectile is

$$\tilde{\sigma}_{cyl} = \frac{1}{4\tau} \int_0^1 u \cos\left(\frac{u^2}{4\tau}\right) du \tag{36a}$$

which readily integrates to

$$\tilde{\sigma}_{cyl} = \frac{1}{2} \sin(4\tau)^{-1} \tag{36b}$$

This result indicates that the nondimensional stress at the origin oscillates between $\pm 1/2$ with initially infinite frequency and diminishing frequency as τ increases.

Cone.- $g_{co}(\eta) = 1 - \eta$

Substituting $g_{co}(\eta) = 1 - \eta$ into equation (25) yields the nondimensional stress at the origin as

$$\tilde{\sigma}_{co} = \frac{1}{4\tau} \int_o^1 u(1 - u)\cos\left(\frac{u^2}{4\tau}\right)du \tag{37a}$$

which, after integration by parts and an appropriate change of variables, becomes

$$\tilde{\sigma}_{co} = \tau^{1/2} \int_o^{(4\tau)^{-1/2}} \sin y^2 \, dy \tag{37b}$$

The integral is the familiar Fresnel Sine Integral which is tabulated in mathematics handbooks.

Sphere.- $g_{sph}(\eta) = (1 - \eta^2)^{1/2}$

The sphere always presents problems in impact analyses; this one not being the exception. Rather than getting nice, clean expressions for the stress at the origin as equations (36b) and (37b) for the cylinder and cone, respectively, the sphere gives a series answer to the integral resulting from substituting $g_{sph}(\eta) = (1 - \eta^2)^{1/2}$ into equation (25), that is,

$$\tilde{\sigma}_{sph} = \frac{1}{4\tau} \int_o^1 u(1 - u^2)^{1/2} \cos\left(\frac{u^2}{4\tau}\right)du \tag{38a}$$

which is evaluated in the appendix as

$$\tilde{\sigma}_{sph} = \frac{1}{4}\pi^{1/2}\sum_{n=0}^{\infty}\frac{(-1)^n(4\tau)^{-(2n+1)}}{\Gamma\left(2n+\frac{5}{2}\right)} \tag{38b}$$

Again in the three examples, only projectile shape has been specified. Selecting the projectile characteristics as before, the comparable non-dimensional stresses at the origin become

$$\bar{\tilde{\sigma}}_{cyl} = \frac{a(1-\nu)}{2zEQ}\sigma_{cyl} = \frac{2}{3}\tilde{\sigma}_{cyl} \tag{39a}$$

$$\bar{\tilde{\sigma}}_{co} = \frac{a(1-\nu)}{2zEQ}\sigma_{co} = 2\tilde{\sigma}_{co} \tag{39b}$$

$$\bar{\tilde{\sigma}}_{sph} = \frac{a(1-\nu)}{2zEQ}\sigma_{sph} = \tilde{\sigma}_{sph} \tag{39c}$$

Equations (39a), (39b), and (39c) combined with equations (36b), (37b), and (38b), respectively, have been evaluated for τ ranging from zero to 1 and are presented in figure 8 to demonstrate the effects of these projectile shapes on the maximum stress at the origin. Note that in all three cases a distinct peak occurs after which the stresses rapidly converge. The peak stress for the cone impact is 1.58 times and for the sphere impact is 1.22 times that of the cylinder. Hence, the peak stress at the origin also indicates that the cone causes larger responses of the plate than either the sphere or cylinder.

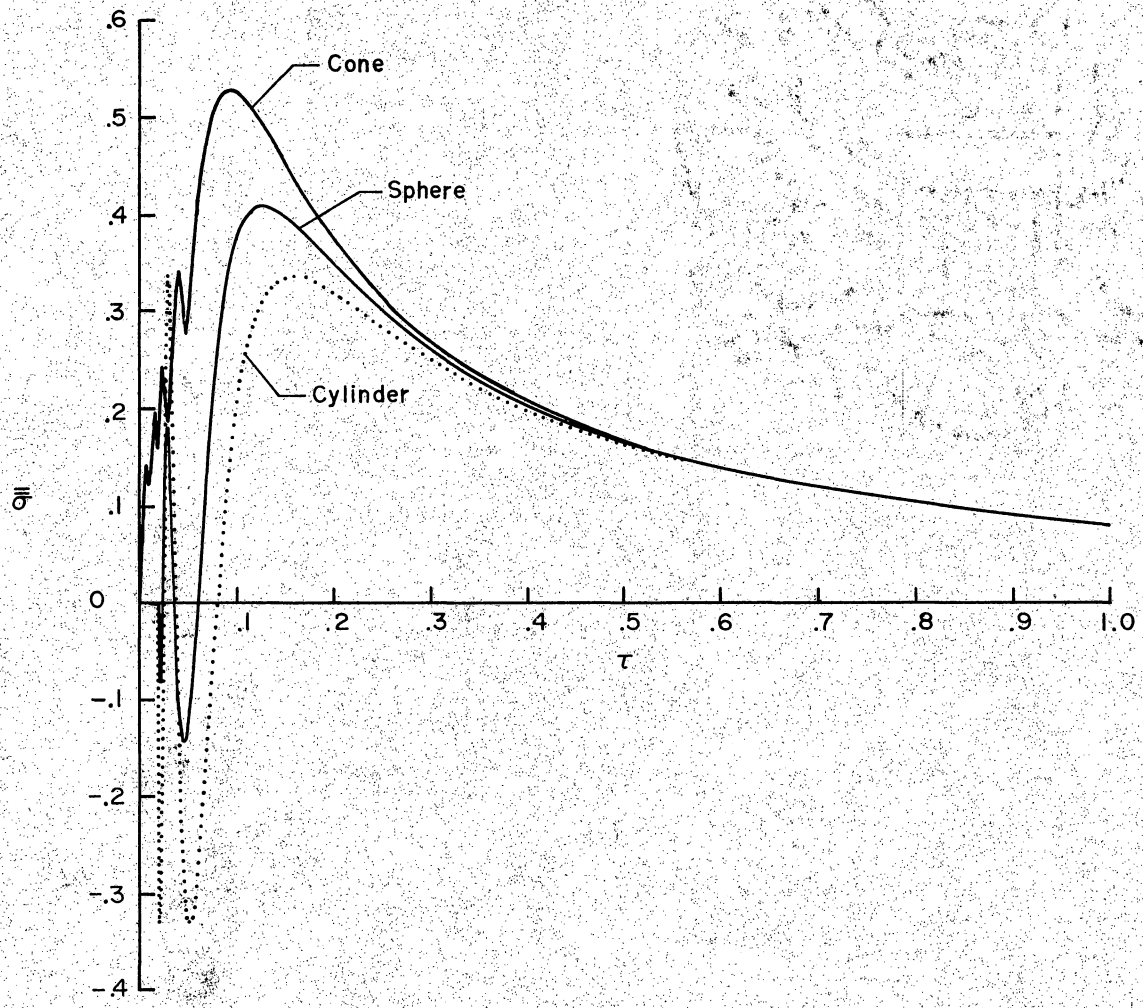

Figure 8.- Variation of the maximum stress at the origin with time for impacting equi-mass and -diameter projectiles.

X. CONCLUDING REMARKS

Linear, elastic, small-deflection plate equations were used to study the response of a single wall structure to the impact of an axisymmetric cometary meteoroid. The analysis assumed that momentum exchange is the primary mechanism, that the time of exchange is instantaneous, and that the momentum of the meteoroid after impact is negligible.

Three particular shapes were studied - cylinder, cone, and sphere. Projectile comparisons based on equal mass, diameter, and total momentum indicate that frangible, low-strength cone projectiles cause significantly higher stresses and larger displacements of the plate at short times after impact than similar sphere and cylinder projectiles.

XI. REFERENCES

1. Sneddon, I. N.: Fourier Transforms. First ed., McGraw-Hill Book Co., Inc., 1951.

2. Medick, M. A.: On Classical Plate Theory and Wave Propagation. J. Appl. Mech., Ser. E., vol. 28, no. 2, June 1961, pp. 223-228.

3. Madden, R.; and Hayduk, R. J.: Equations for the Comparison of the Ballistic Limit of Single and Double Wall Structures. Proposed NASA Technical Note.

4. Cosby, W. A.; and Lyle, R. G.: The Meteoroid Environment and Its Effects on Materials and Equipment. NASA SP-78, 1965.

5. Neswald, R. G.: The Meteoroid Hazard. Space/Aeronautics, vol. 45, no. 5, May 1966, pp. 76-85.

6. Erdélyi, A., ed.: Bateman Manuscript Project. McGraw-Hill Book Co., Inc. (New York), 1954. Vols. I and II - Tables of Integral Transforms.

7. Watson, G. N.: A Treatise on the Theory of Bessel Functions. Second ed., Macmillan Co., 1944.

XII. APPENDIX

EVALUATION OF INTEGRALS

In this thesis the Bateman Manuscript Project Volumes, Tables of Integral Transforms (ref. 6), enabled the evaluation of many difficult integrals that probably would have been intractable had such a set of volumes not been available to the author.

Integral Occurring in the General Stress Expression (eq. (24))

The double-integral expression for the stress at the origin was found to be

$$\tilde{\sigma}_p = \frac{1}{2} \int_0^1 u g_p(u) du \int_0^\infty p J_0(pu) \sin(p^2\tau) dp \tag{A1}$$

The infinite integral can be evaluated from Weber's first exponential integral (ref. 7, p. 394)

$$\int_0^\infty p J_0(up) \exp(-q^2p^2) dp = \frac{1}{2q^2} \exp\left(-\frac{u^2}{4q^2}\right) \tag{A2}$$

By letting $q^2 = i\tau$ and recalling that

$$\exp(-i\theta) = \cos\theta - i \sin\theta \tag{A3}$$

the integral becomes

$$\int_0^\infty J_0(up)\left[\cos(p^2\tau) - i \sin(p^2\tau)\right] p \, dp = \frac{1}{2\tau}\left[\sin\left(\frac{u^2}{4\tau}\right) - i \cos\left(\frac{u^2}{4\tau}\right)\right] \tag{A4}$$

Equating real and imaginary parts yields

$$\int_0^\infty pJ_0(up)\cos(p^2\tau)dp = \frac{1}{2\tau}\sin\left(\frac{u^2}{4\tau}\right) \tag{A5}$$

and

$$\int_0^\infty pJ_0(up)\sin(p^2\tau)dp = \frac{1}{2\tau}\cos\left(\frac{u^2}{4\tau}\right) \tag{A6}$$

Sneddon applied this technique to Weber's second exponential integral and arrived at equation (114) on page 137 (ref. 1), which reduces to the first integral (eq. (A5)) by letting r go to zero. Substituting the second integral (eq. (A6)) into equation (A1) yields equation (25), that is,

$$\tilde{\sigma}_p = \frac{1}{4\tau}\int_0^1 ug_p(u)\cos\left(\frac{u^2}{4\tau}\right)du \tag{A7}$$

Determination of $\bar{g}_p(p)$ (eq. (11)) for the Cone and Sphere

Cone.- The integral

$$\int_0^1 u^2J_0(pu)du \tag{A8}$$

which occurs in the displacement of the plate impacted by a conical projectile (eq. (28)) can be evaluated by changing the integral to a Mellin transform of

$$\begin{aligned} f(u) &= J_0(pu); \quad 0 < u < 1 \\ &= 0 \qquad\quad ; \quad 1 < u < \infty \end{aligned} \tag{A9}$$

By definition the Mellin transform of a function is

$$g(s) = \int_0^\infty f(u)u^{s-1}\,du \tag{A10}$$

On page 326 of reference 6, volume 1, the Mellin transform of

$$\begin{aligned} f(u) &= J_\nu(pu); \quad 0 < u < 1 \\ &= 0 \qquad ; \quad 1 < u < \infty \end{aligned} \tag{A11}$$

is given as

$$\frac{p^\nu}{2^\nu(s+\nu)\Gamma(\nu+1)}\,{}_1F_2\left(\frac{s+\nu}{2};\nu+1,\frac{s+\nu}{2}+1;-\frac{1}{4}p^2\right) \tag{A12}$$

which yields the desired integral if ν is zero and s is 3, that is,

$$\int_0^1 u^2 J_0(pu)du = \frac{1}{3}\,{}_1F_2\left(\frac{3}{2};1,\frac{5}{2};-\frac{1}{4}p^2\right) \tag{A13}$$

Sphere.- The displacement of the plate impacted by a sphere contains the integral (eq. (30))

$$\bar{g}_{sph}(p) = \int_0^1 u(1-u^2)^{1/2} J_0(pu)du \tag{A14}$$

which can also be evaluated as a Mellin transform. On page 327 of reference 6, volume 1, the Mellin transform of

$$f(u) = (1 - u^2)^{\lambda} J_{\nu}(pu); \quad 0 < u < 1$$
$$= 0 \qquad\qquad ; \quad 1 < u < \infty \tag{A15}$$

is given as

$$\frac{p^{\nu} B\left(\lambda + 1, \frac{1}{2} s + \frac{1}{2} \nu\right)}{2^{\nu+1} \Gamma(\nu + 1)} \, {}_1F_2\left(\frac{s + \nu}{2}; \nu + 1, \frac{s + \nu}{2} + 1 + \lambda; -\frac{1}{4} p^2\right) \tag{A16}$$

provided

$$\mathrm{Re}\lambda > -1$$

and

$$\mathrm{Re}s > -\mathrm{Re}\nu$$

By letting ν be zero, s be 2, and λ be 1/2, the desired integral is found to be

$$\int_0^1 u(1 - u^2)^{1/2} J_0(pu)du = \frac{1}{3} \, {}_1F_2\left(1; 1, \frac{5}{2}; -\frac{1}{4} p^2\right) \tag{A17}$$

The identical numerator and denominator parameters of the hypergeometric function cancel, leaving ${}_0F_1\left(\frac{5}{2}; -\frac{1}{4} p^2\right)$. This hypergeometric function is related to the Bessel functions by the relationship

$$J_{\nu}(p) = \frac{\left(\frac{1}{2} p\right)^{\nu}}{\Gamma(\nu + 1)} \, {}_0F_1\left(\nu + 1; -\frac{1}{4} p^2\right) \tag{A18}$$

(ref. 7, p. 100)

Using this relationship, the hypergeometric function can be expressed as

$${}_0F_1\left(\frac{5}{2}; -\frac{1}{4} p^2\right) = 3\left(\frac{\pi}{2}\right)^{1/2} (p)^{-3/2} J_{3/2}(p) \tag{A19}$$

Hence, the final result is

$$\int_0^1 u(1 - u^2)^{1/2} J_0(pu)du = \left(\frac{\pi}{2}\right)^{1/2} p^{-3/2} J_{3/2}(p) \qquad (A20)$$

Short Time Deflections of the Plate ($\tau \ll 1$)

For very small time after the impact, the $\sin p^2\tau$ in the integrands of the deflection integrals (eqs. (27), (29), and (31)) can be approximated by $p^2\tau$ to obtain the short time deflections of the plate.

Cylinder.- The approximation in the cylinder case gives the short time deflection of the plate as

$$\tilde{w}_{cyl}(\eta,\tau \ll 1) = \tau \int_0^\infty J_1(p)J_0(p\eta)dp$$

$$= \tau\eta^{-1/2} \int_0^\infty p^{-1/2} J_1(p)J_0(p\eta)(p\eta)^{1/2}\, dp \qquad (A21)$$

By definition this integral is the zeroth order Hankel transform of the function $p^{-1/2} J_1(p)$. The transform is given on page 14 of reference 6, volume 2, as

$$\int_0^\infty p^{-1/2} J_1(p)J_0(p\eta)(p\eta)^{1/2}\, dp = \begin{cases} \eta^{1/2}; & 0 < \eta < 1 \\ 0 \quad ; & 1 < r < \infty \end{cases} \qquad (A22)$$

The short time deflection of the plate for the cylindrical projectile is

$$\tilde{w}_{cyl}(\eta,\tau \ll 1) = \begin{cases} \tau; & 0 < \eta < 1 \\ 0; & 1 < \eta < \infty \end{cases} \qquad (A23)$$

Cone.- For the conical projectile, the short time deflection expression is

$$\tilde{w}_{co}(\eta,\tau \ll 1) = \tau \int_0^\infty J_1(p)J_o(p\eta)dp$$

$$- \frac{1}{3}\tau \int_0^\infty p\ {}_1F_2\left(\frac{3}{2};1,\frac{5}{2};-\frac{1}{4}p^2\right)J_o(p\eta)dp \qquad (A24)$$

The first integral is the same as in the cylinder case; the second integral can be rewritten as

$$\eta^{-1/2}\int_0^\infty p^{1/2}\,{}_1F_2\left(\frac{3}{2};1,\frac{5}{2};-\frac{1}{4}p^2\right)J_o(p\eta)(p\eta)^{1/2}\,dp \qquad (A25)$$

which by definition is the zeroth order Hankel transform of the function $p^{1/2}\,{}_1F_2\left(\frac{3}{2};1,\frac{5}{2};-\frac{1}{4}p^2\right)$. On page 88 of reference 6, volume 2, the νth order Hankel transform of

$$p^{\nu+\frac{1}{2}}\,{}_1F_2\left(\alpha;\beta,\nu+1;-\frac{1}{4}p^2\right) \qquad (A26)$$

is given as

$$\frac{\Gamma(\nu+1)\Gamma(\beta)}{\Gamma(\alpha)\Gamma(\beta-\alpha)}\,2^{\nu+1}\,\eta^{2\alpha-\nu-\frac{3}{2}}(1-\eta^2)^{\beta-\alpha-1};\quad 0<\eta<1$$

$$0;\quad 1<\eta<\infty \qquad (A27)$$

provided $\mathrm{Re}\nu > -1$ and $\mathrm{Re}\beta > \mathrm{Re}\alpha > 0$.

Since the order in which the numerator and denominator parameters of a hypergeometric function are written makes no difference, the choice of $\nu = 0$, $\alpha = \frac{3}{2}$, and $\beta = \frac{5}{2}$ in the above transform yields the desired integral, that is,

$$\int_0^\infty p^{1/2}\,{}_1F_2\left(\frac{3}{2};1,\frac{5}{2};-\frac{1}{4}p^2\right)J_0(p\eta)(p\eta)^{1/2}\,dp = \begin{cases} 3\eta^{3/2}; & 0 < \eta < 1 \\ 0 \quad ; & 1 < \eta < \infty \end{cases} \tag{A28}$$

This integral plus the integral evaluated for the cylinder case combine (eq. (A24)) to give the short time deflection for a plate impacted by a conical projectile as

$$\tilde{w}_{co}(\eta,\tau \ll 1) = \begin{cases} \tau(1-\eta); & 0 < \eta < 1 \\ 0 \quad ; & 1 < \eta < \infty \end{cases} \tag{A29}$$

Sphere.- Using the short time approximation as before, the deflection for a plate impacted by a sphere is

$$\tilde{w}_{sph}(\eta,\tau \ll 1) = \left(\frac{\pi}{2}\right)^{1/2} \tau \int_0^\infty p^{-1/2}\,J_{3/2}(p)J_0(p\eta)dp \tag{A30}$$

Again rewriting this as a zeroth order Hankel transform

$$\tilde{w}_{sph}(\eta,\tau \ll 1) = \left(\frac{\pi}{2}\right)^{1/2} \tau\eta^{-1/2} \int_0^\infty p^{-1}\,J_{3/2}(p)J_0(p\eta)(p\eta)^{1/2}\,dp \tag{A31}$$

the integral can be evaluated from the νth order Hankel transform of the function

$$p^{\nu-\mu+\frac{1}{2}} J_\mu(ap) \tag{A32}$$

given as

$$\frac{2^{\nu-\mu+1}\eta^{\nu+\frac{1}{2}}}{\Gamma(\mu-\nu)a^\mu}(a^2-\eta^2)^{\mu-\nu-1};\quad 0<\eta<a$$
$$0;\quad a<\eta<\infty \tag{A33}$$

on page 48 of reference 6, volume 2, provided $a > 0$ and $-1 < \mathrm{Re}\nu < \mathrm{Re}\mu$. In this case $\nu = 0$, $\mu = \frac{3}{2}$, and $a = 1$. The desired integral is

$$\int_0^\infty p^{-1} J_{3/2}(p) J_0(p\eta)(p\eta)^{1/2}\,dp = \begin{cases} \left(\frac{2}{\pi}\right)^{1/2} \eta^{1/2}(1-\eta^2)^{1/2}; & 0<\eta<1 \\ 0 \qquad\qquad\qquad\quad ; & 1<\eta<\infty \end{cases} \tag{A34}$$

which gives

$$\tilde{w}_{sph}(\eta, \tau \ll 1) = \begin{cases} \tau(1-\eta^2)^{1/2}; & 0<\eta<1 \\ 0 \qquad\qquad ; & 1<\eta<\infty \end{cases} \tag{A35}$$

for the short time deflection of a plate after being impacted by a spherical projectile.

Maximum Stress in the Sphere Case (eq. (38a))

The integral for the stress at the axis of symmetry for the sphere case is

$$\tilde{\sigma}_{sph} = \frac{1}{4\tau}\int_0^1 u(1-u^2)^{1/2}\cos\left(\frac{u^2}{4\tau}\right)du \tag{A36}$$

Again, this integral can be handled as a Mellin transform if a change of variables is made. Let $x = u^2$ and $b = \frac{1}{4\tau}$, then

$$\tilde{\sigma}_{sph} = \frac{1}{8\tau} \int_0^1 (1 - x)^{1/2} \cos(bx)dx \tag{A37}$$

On page 320 of reference 6, volume 1, the Mellin transform of

$$\begin{aligned} f(x) &= (1 - x)^{\nu-1} \cos(bx); \quad 0 < x < 1 \\ &= 0 \qquad\qquad\qquad ; \quad 1 < x < \infty \\ \mathrm{Re}\nu &> 0 \end{aligned} \tag{A38}$$

is given as

$$\frac{1}{2} B(s,\nu)\left[{}_1F_1(s;s + \nu;ib) + {}_1F_1(s;s + \nu;-ib)\right] \tag{A39}$$

for $\mathrm{Re}s > 0$. By letting ν be $\frac{3}{2}$ and s be 1, the desired integral becomes

$$\int_0^1 (1 - x)^{1/2} \cos(bx)dx = \frac{1}{3}\left[{}_1F_1\left(1;\frac{5}{2};ib\right) + {}_1F_1\left(1;\frac{5}{2};-ib\right)\right] \tag{A40}$$

The confluent hypergeometric function is the power series

$$\begin{aligned} {}_1F_1(a;b;z) &= 1 + \frac{a}{b}\frac{z}{1!} + \frac{a(a + 1)}{b(b + 1)}\frac{z^2}{2!} + \cdots \\ &= \sum_{n=0}^{\infty} \frac{(a)_n}{(b)_n}\frac{z^n}{n!} \end{aligned} \tag{A41}$$

where Pochammer's notation used for the numerator and denominator parameters is

$$(a)_n = a(a + 1)(a + 2) \ldots (a + n - 1)$$

and (A42)

$$(a)_o = 1$$

Adding the confluent hypergeometric functions of equation (A25) term by term eliminates all the imaginary terms. In general, then

$${}_1F_1(a;b;iz) + {}_1F_1(a;b;-iz) = 2 \sum_{n=0}^{\infty} (-1)^n \frac{(a)_{2n}}{(b)_{2n}} \frac{z^{2n}}{(2n)!} \tag{A43}$$

These results give

$$\tilde{\sigma}_{sph} = \frac{1}{12\tau} \sum_{n=0}^{\infty} (-1)^n \frac{(1)_{2n}}{\left(\frac{5}{2}\right)_{2n}} \frac{(4\tau)^{-2n}}{(2n)!} \tag{A44}$$

which reduces to (eq. (38b))

$$\tilde{\sigma}_{sph} = \frac{1}{4} \pi^{1/2} \sum_{n=0}^{\infty} \frac{(-1)^n (4\tau)^{-(2n+1)}}{\Gamma\left(2n + \frac{5}{2}\right)} \tag{A45}$$

The vita has been removed from the scanned document

THE RESPONSE OF A SINGLE WALL SPACE STRUCTURE TO IMPACT BY COMETARY METEOROIDS OF VARIOUS SHAPES

By

Robert J. Hayduk

ABSTRACT

Linear, small-deflection plate theory is used to study the stress at the contact axis and the deflection of an infinite plate caused by the impact of an axisymmetric cometary meteoroid. The analysis assumes that momentum exchange is the primary mechanism, that the time of exchange is instantaneous, and that the momentum of the meteoroid is negligible after impact. The stress at the origin is reduced to a single definite integral and the deflection to the Hankel inversion integral, both requiring definition of the particular projectile before further evaluation. A particular cometary meteoroid is mathematically represented in the analysis by its projected momentum per unit area onto the plate.

The three specific shapes studied are the usual projectile shapes used in hypervelocity laboratories - cylinder, cone, and sphere - even though the analysis is not intended for the high-strength, high-density laboratory projectiles. Projectile comparisons based on equal mass, diameter, and total momentum indicate that frangible, low-strength cone projectiles cause significantly higher stresses and larger displacements of the plate at short times after impact than similar sphere and cylinder projectiles.